

Data-Driven Optimization: Theory, Algorithms, and Applications (Part II)

Xianchao Xiu

Department of Automation



Mathematical Optimization Society, May 16-19, 2025

Outline

Introduction

Hyperspectral Denoising

Infrared Small Target Detection

Conclusions

Introduction

- ▶ Iterative shrinkage thresholding algorithm (ISTA)

$$\min_{x \in \mathbb{R}^n} \frac{1}{2} \|Ax - y\|_2^2 + \lambda \|x\|_1$$

- ▶ Step 1: Compute gradient

$$r^{k+1} = x^k - \rho A^\top (Ax^k - y)$$

- ▶ Step 2: Compute shrinkage

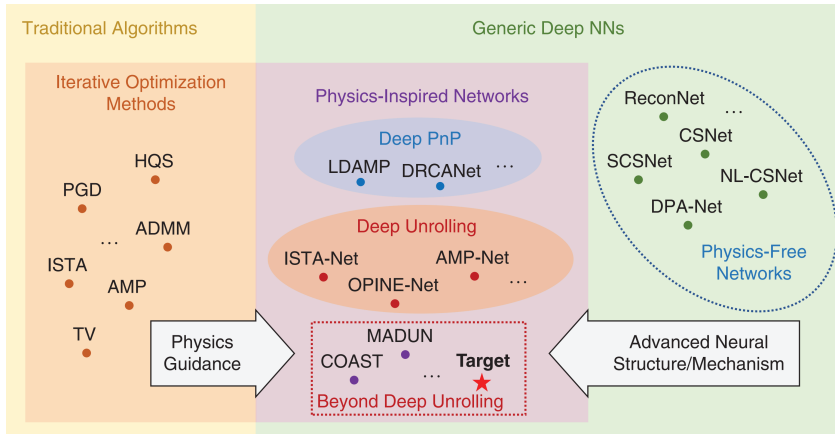
$$x^{k+1} = \arg \min_{x \in \mathbb{R}^n} \frac{1}{2} \|x - r^{k+1}\|_2^2 + \lambda \|x\|_1$$

- ▶ Gregor-LeCun, Learning Fast Approximations of Sparse Coding, ICML, 2010

$$x^{(k+1)} = h_\theta(x^k - \rho A^\top (Ax^k - y))$$

Introduction

- Zhang-Che-Xiong et al, Physics-Inspired Compressive Sensing: Beyond Deep Unrolling, IEEE SPM, 2023



Outline

Introduction

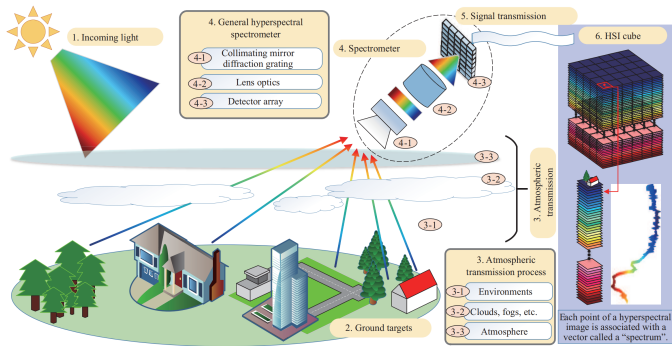
Hyperspectral Denoising

Infrared Small Target Detection

Conclusions

HSI

- ▶ Hyperspectral image (HSI): Rich spectral and spatial information

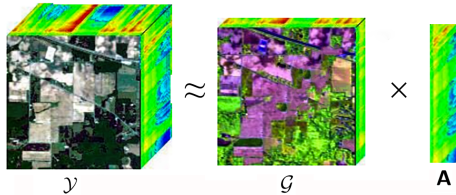


- ▶ Board applications: Agriculture, astronomy, geosciences, medicine
- ▶ Various tasks: Denoising, classification, detection, fusion, unmixing
- ▶ <https://github.com/xianchaoxiu/Hyperspectral-Imaging>

Motivation

- ▶ General subspace tensor representation framework

$$\begin{aligned} (\text{P}) \quad & \min_{\mathcal{G}, A} \frac{1}{2} \|\mathcal{Y} - \mathcal{G} \times_3 A\|_{\text{F}}^2 + \lambda \Omega(\mathcal{G}) \\ \text{s.t. } & A^\top A = I \end{aligned}$$



- ▶ What are the advantages of tensor modeling?
 - ▶ Excellent data representation
 - ▶ Various tensor decomposition
 - ▶ (possibly) Low computational complexity

Motivation

- Xiong-Zhou-Tao et al, SMDS-Net: Model Guided Spectral-Spatial Network for Hyperspectral Image Denoising, [IEEE TIP](#), 2022

$$(P) \quad \min_{\mathcal{G}, A} \frac{1}{2} \|\mathcal{Y} - \mathcal{G} \times_3 A\|_F^2 + \lambda \Omega(\mathcal{G})$$

$$\text{s.t. } A^\top A = I$$

↓

$$\min_{\mathcal{G}, \mathcal{B}_i, A} \frac{1}{2} \|\mathcal{Y} - \mathcal{G} \times_3 A\|_F^2 + \lambda \sum_i (\phi(\mathcal{G}, \mathcal{B}_i) + \gamma_1 \|\mathcal{B}_i\|_1)$$

$$\text{s.t. } A^\top A = I$$

- Multidimensional representation

$$\phi(\mathcal{G}, \mathcal{B}_i) = \frac{1}{2} \|\mathcal{R}_i \mathcal{G} - \mathcal{B}_i \times_1 D_1 \times_2 D_2 \times_3 D_3\|_F^2$$

- How to characterize priors? How to develop algorithms?

Model

- Sparse tensor aided representation (STAR)

$$\begin{aligned} (\text{P}) \quad & \min_{\mathcal{G}, A} \frac{1}{2} \|\mathcal{Y} - \mathcal{G} \times_3 A\|_{\text{F}}^2 + \lambda \Omega(\mathcal{G}) \\ \text{s.t. } & A^\top A = I \end{aligned}$$

↓

$$\begin{aligned} (\text{STAR}) \quad & \min_{\mathcal{G}, \mathcal{B}_i, A} \frac{1}{2} \|\mathcal{Y} - \mathcal{G} \times_3 A\|_{\text{F}}^2 + \lambda \sum_i (\phi(\mathcal{G}, \mathcal{B}_i) + \gamma_1 \|\mathcal{B}_i\|_1 + \gamma_2 \|\mathcal{B}_i\|_*) \\ \text{s.t. } & A^\top A = I \end{aligned}$$

↓

$$\begin{aligned} (\text{STAR-S}) \quad & \min_{\mathcal{G}, \mathcal{S}, \mathcal{B}_i, A} \frac{1}{2} \|\mathcal{Y} - \mathcal{G} \times_3 A - \mathcal{S}\|_{\text{F}}^2 + \mu \|\mathcal{S}\|_1 \\ & + \lambda \sum_i (\phi(\mathcal{G}, \mathcal{B}_i) + \gamma_1 \|\mathcal{B}_i\|_1 + \gamma_2 \|\mathcal{B}_i\|_*) \\ \text{s.t. } & A^\top A = I \end{aligned}$$

Algorithm

- ▶ Alternating direction method of multipliers (ADMM)

$$\min_{\mathcal{G}, \mathcal{B}_i, \mathcal{L}_i, A} \frac{1}{2} \|\mathcal{Y} - \mathcal{G} \times_3 A\|_F^2 + \lambda \sum_i (\phi(\mathcal{G}, \mathcal{B}_i) + \gamma_1 \|\mathcal{B}_i\|_1 + \gamma_2 \|\mathcal{L}_i\|_*)$$

s.t. $A^\top A = I$, $\mathcal{L}_i = \mathcal{B}_i$

↓

$$\begin{aligned} L_\beta(\mathcal{G}, \mathcal{B}_i, \mathcal{L}_i, A, \mathcal{P}_i) &= \frac{1}{2} \|\mathcal{Y} - \mathcal{G} \times_3 A\|_F^2 \\ &+ \lambda \sum_i (\phi(\mathcal{G}, \mathcal{B}_i) + \gamma_1 \|\mathcal{B}_i\|_1 + \gamma_2 \|\mathcal{L}_i\|_*) \\ &+ \langle \mathcal{P}_i, \mathcal{L}_i - \mathcal{B}_i \rangle + \frac{\beta}{2} \|\mathcal{L}_i - \mathcal{B}_i\|_F^2 \end{aligned}$$

- ▶ Note that $A^\top A = I$ is preserved

STAR-Net

- ▶ Update \mathcal{G} -block

$$\begin{aligned}\mathcal{G}^{k+1} = & \arg \min_{\mathcal{G}} \frac{1}{2} \|\mathcal{Y} - \mathcal{G} \times_3 A^k\|_F^2 \\ & + \frac{\lambda}{2} \sum_i \|\mathcal{R}_i \mathcal{G} - \mathcal{B}_i^k \times_1 D_1 \times_2 D_2 \times_3 D_3\|_F^2 \\ & \Downarrow\end{aligned}$$

$$\begin{aligned}\mathcal{G}^{k+1} = & (\mathcal{I} + \lambda \sum_i \mathcal{R}_i^\top \mathcal{R}_i)^{-1} (\lambda \sum_i \mathcal{R}_i^\top \mathcal{B}_i^k \times_1 D_1 \times_2 D_2 \times_3 D_3 + \mathcal{Y} \times_3 A^{k\top}) \\ & \Downarrow\end{aligned}$$

$$\mathcal{G}^{k+1} = \mathcal{E}_1 * \mathcal{E}_2$$

↓

$$\mathcal{G}^{k+1} = \text{LargNet}(\mathcal{E}_1, \mathcal{E}_2)$$

STAR-Net

- ▶ Update \mathcal{B}_i -block

$$\mathcal{B}_i^{k+1} = \arg \min_{\mathcal{B}_i} \frac{\lambda}{2} \|\mathcal{R}_i \mathcal{G}^{k+1} - \mathcal{B}_i \times_1 D_1 \times_2 D_2 \times_3 D_3\|_F^2$$

$$+ \frac{\beta}{2} \|\mathcal{L}_i^k - \mathcal{B}_i + \mathcal{P}_i^k / \beta\|_F^2 + \lambda \gamma_1 \|\mathcal{B}_i\|_1$$

↓

$$\mathcal{B}_i^{k+1} = \arg \min_{\mathcal{B}_i} \frac{1}{2} \|(\beta \mathcal{I} + \lambda \mathcal{I} \times_1 D_1 \times_2 D_2 \times_3 D_3) \mathcal{B}_i\|_F^2$$

$$- (\lambda \mathcal{R}_i \mathcal{G}^{k+1} + \beta \mathcal{L}_i^k + \mathcal{P}_i^k)\|_F^2 + \lambda \gamma_1 \|\mathcal{B}_i\|_1$$

↓

$$\mathcal{B}_i^{k+1} = \text{sgn}(\mathcal{F}_i) \circ \text{ReLU}(|\mathcal{F}_i| - \lambda \gamma_1 / \nu)$$

↓

$$\mathcal{B}_i^{k+1} = \text{ShrinkNet}(\mathcal{F}_i, \lambda \gamma_1 / \nu)$$

STAR-Net

- ▶ Update A -block

$$A^{k+1} = \arg \min_{A^\top A = I} \frac{1}{2} \|\mathcal{Y} - \mathcal{G}^{k+1} \times_3 A\|_F^2$$

↓

$$A^{k+1} = UV^\top$$

↓

$$A^{k+1} = \text{LargNet}(U, V^\top)$$

- ▶ Update \mathcal{P}_i -block

$$\mathcal{P}_i^{k+1} = \mathcal{P}_i^k + \beta(\mathcal{L}_i^{k+1} - \mathcal{B}_i^{k+1})$$

↓

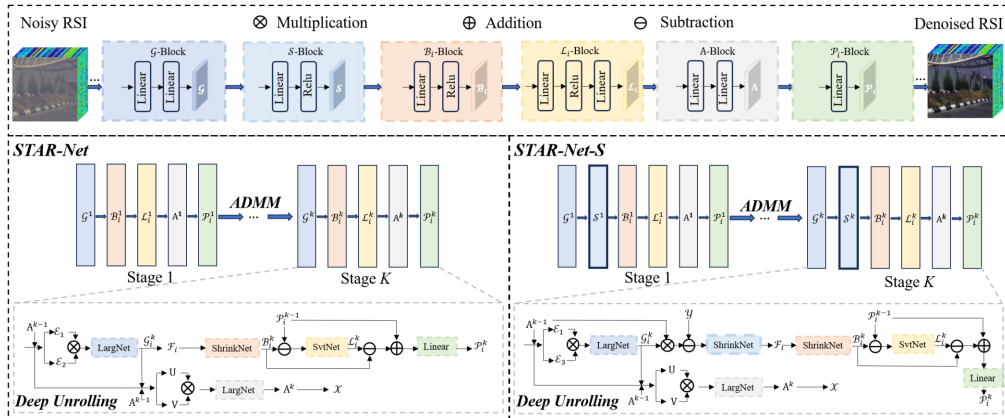
$$\mathcal{P}_i^{k+1} = \text{Linear}(\Theta_i)$$

STAR-Net

- ▶ **Input:** Noisy HSI \mathcal{Y} , parameters $\lambda, \beta, \gamma_1, \gamma_2, \nu$
- ▶ **Initialize:** $(\mathcal{G}^0, \mathcal{B}_i^0, \mathcal{L}_i^0, \mathcal{A}^0, \mathcal{P}_i^0)$
- ▶ **While** $k = 1, \dots, K$ **do**
 - ▶ Update \mathcal{G} -block by
$$\mathcal{G}^{k+1} = \text{LargNet}(\mathcal{E}_1, \mathcal{E}_2)$$
 - ▶ Update \mathcal{B}_i -block by
$$\mathcal{B}_i^{k+1} = \text{ShrinkNet}(\mathcal{F}_i, \lambda\gamma_1/\nu)$$
 - ▶ Update \mathcal{L}_i -block by
$$\mathcal{L}_i^{k+1} = \text{SvtNet}(\mathcal{B}_i^{k+1} - \mathcal{P}_i^k/\beta, \lambda\gamma_2/\beta)$$
 - ▶ Update \mathcal{A} -block by
$$\mathcal{A}^{k+1} = \text{LargNet}(U, V^\top)$$
 - ▶ Update \mathcal{P}_i -block by
$$\mathcal{P}_i^{k+1} = \text{Linear}(\Theta_i)$$
- ▶ **Output:** Denoised HSI $\mathcal{X} = \mathcal{G}^{k+1} \times_3 \mathcal{A}^{k+1}$

Architecture

► Our proposed STAR-Net and STAR-Net-S



Setup

- ▶ Compared methods
 - ▶ BM4D: Maggioni-Katkovnik-Egiazarian et al, IEEE TIP, 2012
 - ▶ LLRT: Chang-Yan-Zhong, CVPR, 2017
 - ▶ LRTDTV: Wang-Chen-Han et al, RS, 2017
 - ▶ NGMeet: He-Yao-Li-Yokoya et al, IEEE TPAMI, 2022
 - ▶ NLSSR: Zha-Wen-Yuan et al, IEEE TGRS, 2023
 - ▶ FastHyMix: Zhuang-Ng, IEEE TNNLS, 2023
 - ▶ HSI-SDeCNN: Maffei-Haut-Paoletti et al, IEEE TGRS, 2020
 - ▶ SMDS-Net: Xiong-Zhou-Tao et al, IEEE TIP, 2022
 - ▶ Eigen-CNN: Zhuang-Ng-Gao et al, IEEE TGRS, 2024
 - ▶ RCILD: Peng-Wang-Cao et al, IEEE TGRS, 2024
- ▶ Implementation details
 - ▶ Training loss: $L = \|\text{STAR-Net}(\mathcal{Y}) - \mathcal{X}\|_F^2$
 - ▶ Training dataset: 100 HSIs from ICVL, data augmentation
 - ▶ Testing dataset: ICVL, Washington DC Mall
 - ▶ Hyperparameters: Learning rate=0.005, batch=2, epoch=300, K=6, dictionary=[9, 9, 9]
 - ▶ Training parameters: $\lambda, \beta, \mu, \gamma_1, \gamma_2, D_1, D_2, D_3$

Synthetic

► Quantitative comparisons on ICVL with under Gaussian noise

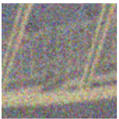
σ	Index	Noisy	BM4D	LLRT	LRTDTV	NGMeet	NLSSR	FastHyMix	HSI-SDeCNN	SMDS-Net	Eigen-CNN	RCILD	STAR-Net	STAR-Net-S
10	PSNR \uparrow	29.018	42.987	39.810	43.882	42.383	45.928	43.628	41.519	46.371	47.321	42.458	47.286	47.345
	SSIM \uparrow	0.521	0.973	0.962	0.979	0.968	0.984	0.988	0.969	0.985	0.989	0.987	0.988	0.989
	SAM \downarrow	0.229	0.080	0.045	0.077	0.074	0.066	0.035	0.075	0.028	0.032	0.044	0.025	0.025
	ERGAS \downarrow	243.021	36.420	59.279	44.893	34.764	28.026	24.893	61.289	20.056	25.355	25.800	18.124	17.951
30	PSNR \uparrow	21.591	37.630	34.250	38.245	36.791	41.629	38.286	36.840	42.337	41.491	38.514	42.435	42.500
	SSIM \uparrow	0.146	0.930	0.921	0.877	0.915	0.968	0.966	0.926	0.972	0.963	0.971	0.972	0.972
	SAM \downarrow	0.535	0.142	0.084	0.149	0.139	0.084	0.068	0.124	0.040	0.060	0.067	0.039	0.038
	ERGAS \downarrow	729.026	62.662	40.725	69.464	60.101	41.388	48.675	103.084	32.393	49.458	49.362	32.056	31.862
50	PSNR \uparrow	18.402	35.242	32.067	33.659	34.399	39.713	35.397	34.342	37.481	36.579	35.838	39.853	39.963
	SSIM \uparrow	0.042	0.888	0.899	0.862	0.887	0.955	0.941	0.893	0.907	0.879	0.951	0.956	0.956
	SAM \downarrow	0.779	0.190	0.107	0.195	0.177	0.109	0.096	0.134	0.066	0.106	0.092	0.050	0.047
	ERGAS \downarrow	1215.105	81.133	54.869	110.351	80.585	53.811	68.681	136.304	55.786	85.426	68.945	43.362	42.923
70	PSNR \uparrow	18.126	33.586	30.746	30.565	32.389	37.450	33.377	32.794	37.197	32.194	33.980	37.342	38.237
	SSIM \uparrow	0.038	0.844	0.852	0.762	0.858	0.934	0.915	0.855	0.923	0.752	0.930	0.943	0.943
	SAM \downarrow	0.897	0.231	0.214	0.304	0.217	0.128	0.120	0.186	0.066	0.154	0.098	0.058	0.055
	ERGAS \downarrow	1701.060	97.267	66.690	163.788	97.309	65.893	88.790	173.430	58.223	126.017	89.340	57.341	52.261
Average	PSNR \uparrow	21.784	37.361	34.218	36.588	36.490	41.180	37.672	36.374	40.846	39.396	37.697	41.729	42.011
	SSIM \uparrow	0.187	0.909	0.909	0.870	0.907	0.960	0.953	0.911	0.947	0.896	0.960	0.965	0.965
	SAM \downarrow	0.610	0.161	0.113	0.181	0.152	0.097	0.080	0.130	0.050	0.088	0.075	0.043	0.041
	ERGAS \downarrow	972.053	69.370	55.391	97.124	68.190	47.280	57.760	118.527	41.614	71.564	58.362	37.721	36.249

Synthetic

► Visualization results



(a) PSNR(dB)



(b) 18.402



(c) 35.242



(d) 32.067



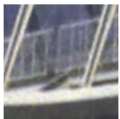
(e) 33.659



(f) 34.399



(g) 39.713



(h) 35.397



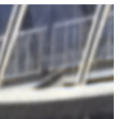
(i) 34.342



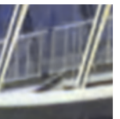
(j) 37.481



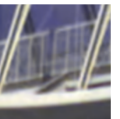
(k) 36.579



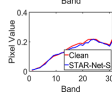
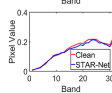
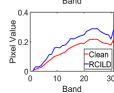
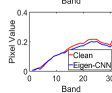
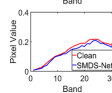
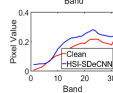
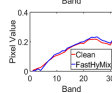
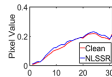
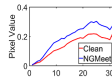
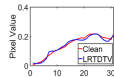
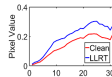
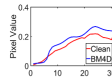
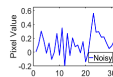
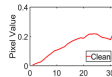
(l) 35.838



(m) 39.853



(n) 39.963



Synthetic

► Quantitative comparisons on PaviaU with under Gaussian noise

σ	Index	Noisy	BM4D	LLRT	LRTDTV	NGMeet	NLSSR	FastHyMix	HSI-SDeCNN	SMDS-Net	Eigen-CNN	RCILD	STAR-Net	STAR-Net-S
10	PSNR \uparrow	29.181	34.044	30.671	31.796	36.493	35.419	39.646	38.509	35.882	39.660	40.509	40.881	41.172
	SSIM \uparrow	0.654	0.902	0.821	0.856	0.933	0.925	0.968	0.953	0.938	0.969	0.962	0.971	0.971
	SAM \downarrow	0.221	0.108	0.159	0.141	0.084	0.092	0.060	0.067	0.068	0.060	0.056	0.049	0.049
	ERGAS \downarrow	157.975	77.328	116.590	102.736	60.251	67.076	44.100	48.351	67.165	44.016	44.690	40.944	39.927
30	PSNR \uparrow	21.409	28.398	30.394	31.756	30.448	33.835	32.960	32.236	30.010	33.028	35.947	35.637	35.976
	SSIM \uparrow	0.237	0.746	0.809	0.855	0.818	0.901	0.919	0.849	0.929	0.922	0.899	0.935	0.936
	SAM \downarrow	0.580	0.202	0.165	0.141	0.610	0.111	0.125	0.134	0.077	0.124	0.090	0.074	0.073
	ERGAS \downarrow	473.723	147.139	120.494	103.199	119.247	80.904	96.429	98.539	73.304	95.860	69.178	68.764	66.131
50	PSNR \uparrow	18.760	26.159	27.022	31.648	27.756	31.750	31.909	29.198	31.748	32.031	31.416	33.227	33.243
	SSIM \uparrow	0.114	0.650	0.666	0.850	0.722	0.856	0.897	0.757	0.878	0.899	0.831	0.898	0.902
	SAM \downarrow	0.816	0.259	0.242	0.196	0.220	0.140	0.138	0.182	0.098	0.136	0.150	0.093	0.092
	ERGAS \downarrow	789.831	188.949	177.238	104.514	162.735	103.138	105.438	138.135	104.315	104.304	115.949	89.223	88.743
70	PSNR \uparrow	16.705	24.940	26.626	30.644	26.281	30.180	31.087	27.435	30.989	31.097	30.560	31.658	31.694
	SSIM \uparrow	0.064	0.595	0.643	0.820	0.659	0.814	0.876	0.694	0.859	0.872	0.779	0.868	0.868
	SAM \downarrow	0.971	0.298	0.254	0.160	0.265	0.166	0.150	0.215	0.113	0.150	0.157	0.105	0.105
	ERGAS \downarrow	1105.483	216.652	185.492	117.070	193.479	122.756	114.277	169.228	113.503	114.060	126.980	106.249	105.060
Average	PSNR \uparrow	21.514	28.385	28.678	31.461	30.245	32.796	33.901	31.844	32.157	33.954	34.608	35.351	35.521
	SSIM \uparrow	0.267	0.723	0.735	0.845	0.783	0.874	0.915	0.813	0.901	0.915	0.868	0.918	0.919
	SAM \downarrow	0.647	0.217	0.205	0.159	0.295	0.127	0.118	0.149	0.089	0.118	0.113	0.080	0.080
	ERGAS \downarrow	631.753	157.517	149.953	106.880	133.928	93.468	90.061	113.563	89.572	89.560	89.199	76.295	74.965

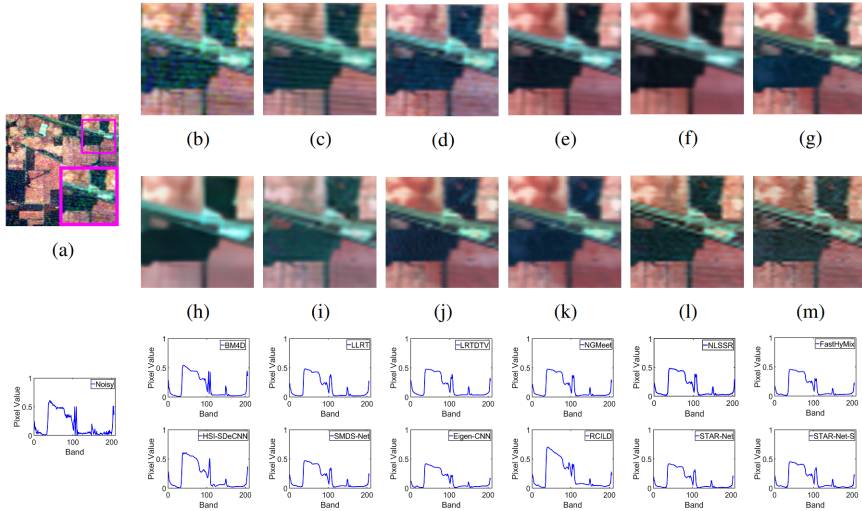
Synthetic

► Quantitative comparisons with non-Gaussian noise

Datasets	Index	Noisy	BM4D	LLRT	LRTDTV	NGMeet	NLSSR	FastHyMix	HSI-SDeCNN	SMDS-Net	Eigen-CNN	RCILD	STAR-Net	STAR-Net-S
ICVL	PSNR ↑	11.695	21.274	19.308	22.587	21.916	20.305	23.319	22.033	23.573	23.436	22.832	23.767	23.847
	SSIM ↑	0.070	0.549	0.331	0.743	0.516	0.417	0.779	0.593	0.754	0.729	0.812	0.840	0.843
	SAM ↓	0.623	0.178	0.262	0.169	0.205	0.233	0.154	0.181	0.097	0.163	0.158	0.097	0.096
	ERGAS ↓	715.955	247.539	319.053	233.654	247.198	256.319	205.134	237.444	184.877	201.632	200.985	180.920	179.610
PaviaU	PSNR ↑	11.200	19.846	20.828	21.977	21.262	22.119	24.363	21.142	22.360	22.434	21.594	22.372	22.558
	SSIM ↑	0.079	0.482	0.540	0.655	0.576	0.714	0.761	0.595	0.722	0.736	0.738	0.728	0.746
	SAM ↓	0.839	0.364	0.316	0.265	0.322	0.260	0.282	0.270	0.205	0.251	0.239	0.205	0.201
	ERGAS ↓	912.728	405.510	394.990	354.904	352.518	259.708	272.636	367.037	264.036	315.859	260.234	263.723	259.505
Average	PSNR ↑	11.448	20.560	20.068	22.282	21.589	21.212	23.841	21.587	22.966	22.935	22.213	23.069	23.202
	SSIM ↑	0.075	0.516	0.436	0.699	0.546	0.565	0.770	0.594	0.738	0.732	0.775	0.784	0.794
	SAM ↓	0.731	0.271	0.289	0.217	0.264	0.246	0.218	0.226	0.151	0.207	0.199	0.151	0.148
	ERGAS ↓	814.342	326.524	357.021	294.279	299.858	258.014	238.885	302.241	224.456	258.745	230.609	222.321	219.557

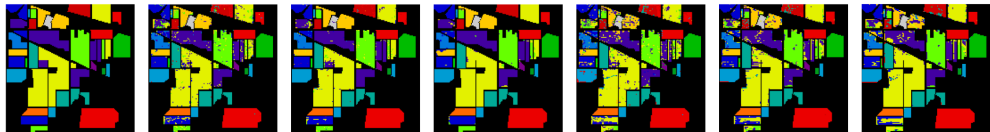
Real-world

► Case study on Indian Pines



Real-world

► Classification



(a)

(b)

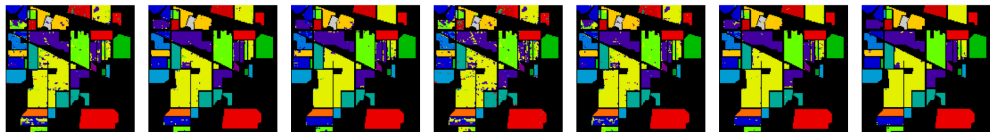
(c)

(d)

(e)

(f)

(g)



(h)

(i)

(j)

(k)

(l)

(m)

(n)

Discussion

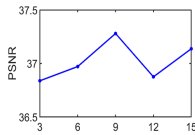
▶ Testing runtime

Datasets	BM4D	LLRT	LRTDTV	NGMeet	NLSSR	FastHyMix	HSI-SDeCNN	SMDS-Net	Eigen-CNN	RCILD	STAR-Net	STAR-Net-S
ICVL	561.307	888.305	136.796	335.265	206.964	8.555	11.093	105.109	6.478	24.743	107.552	107.958
PaviaU	1123.815	2581.424	354.911	716.722	491.568	82.029	60.522	349.292	11.361	30.706	337.133	341.220

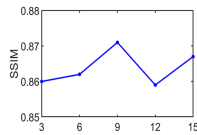
▶ Number of parameters

Methods	FastHyMix	HSI-SDeCNN	SMDS-Net	Eigen-CNN	RCILD	STAR-Net	STAR-Net-S
#Parameters	/	1892100	5103	/	2892288	27702	28487

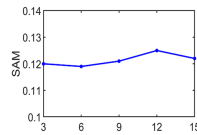
▶ Number of iterations



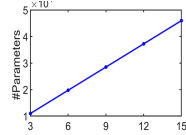
(a) PSNR



(b) SSIM



(c) SAM



(d) #Parameters

Outline

Introduction

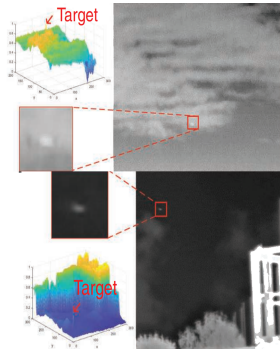
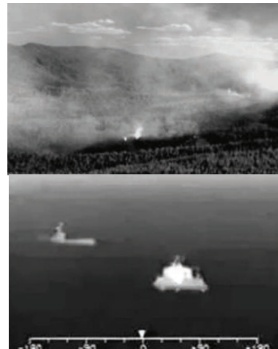
Hyperspectral Denoising

Infrared Small Target Detection

Conclusions

ISTD

- ▶ Infrared small target detection (ISTD)

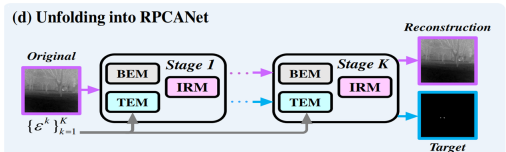
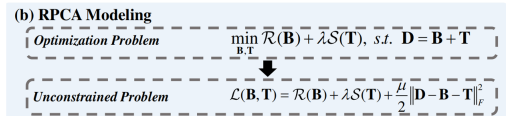
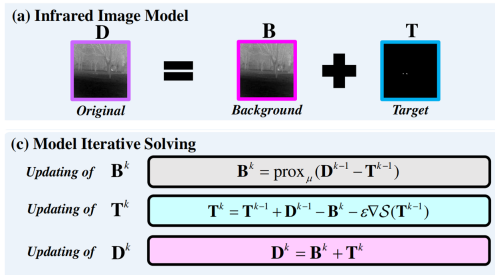


- ▶ Difficulties: Small size, low SNR, weak contrast
- ▶ Advantages: Strong concealment, good anti-interference
- ▶ It is an urgent need in aerospace

Motivation

- Wu-Zhang-Li et al, RPCANet: Deep Unfolding RPCA Based Infrared Small Target Detection, [WACV](#), 2024

$$\begin{aligned} & \min_{B, T} \|B\|_* + \lambda \|T\|_1 \\ \text{s.t. } & D = B + T \end{aligned}$$



Model

- ▶ From RPCANet to L-RPCANet

$$\min_{B, T} \|B\|_* + \lambda \|T\|_1$$

$$\text{s.t. } D = B + T$$

↓

$$\min_{B, T, N} \|B\|_* + \lambda \|T\|_1 + \mu \|N\|_F^2$$

$$\text{s.t. } D = B + T + N$$

↓

$$\min_{B, T, N} \mathcal{R}(B) + \lambda \mathcal{S}(T) + \mu \mathcal{G}(N)$$

$$\text{s.t. } D = B + T + N$$

- ▶ Unconstrained version

$$\mathcal{L}(B, T, N) = \mathcal{R}(B) + \lambda \mathcal{S}(T) + \mu \mathcal{G}(N) + \frac{\alpha}{2} \|D - B - T - N\|_F^2$$

Update B

- Background estimation module + squeeze-and-excitation network (SEBEM)

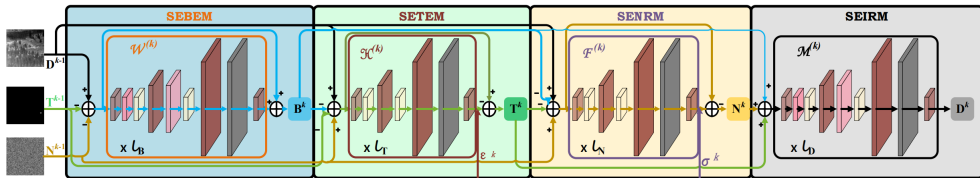
$$B^k = \arg \min_B \mathcal{R}(B) + \frac{\alpha}{2} \|D^{k-1} - B - T^{k-1} - N^{k-1}\|_F^2$$

↓

$$B^k = \text{prox}_\alpha(D^{k-1} - T^{k-1} - N^{k-1})$$

↓

$$B^k = D^{k-1} - T^{k-1} - N^{k-1} + \mathcal{W}^k(D^{k-1} - T^{k-1} - N^{k-1})$$



Update T

- Target estimation module + squeeze-and-excitation network (SETEM)

$$T^k = \arg \min_T \lambda \mathcal{S}(T) + \frac{\alpha}{2} \|D^{k-1} - B^k - T - N^{k-1}\|_F^2$$

↓

$$T^k = \arg \min_T \frac{\lambda L_S}{2} \|T - T^{k-1} + \frac{1}{L_S} \nabla \mathcal{S}(T^{k-1})\|_F^2 + \frac{\alpha}{2} \|D^{k-1} - B^k - T - N^{k-1}\|_F^2$$

↓

$$T^k = \frac{\lambda L_S}{\lambda L_S + \alpha} T^{k-1} + \frac{\alpha}{\lambda L_S + \alpha} (D^{k-1} - B^k - N^{k-1}) - \frac{\lambda}{\lambda L_S + \alpha} \nabla \mathcal{S}(T^{k-1})$$

↓

$$T^k = \gamma T^{k-1} + (1 - \gamma)(D^{k-1} - B^k - N^{k-1}) - \varepsilon \nabla \mathcal{S}(T^{k-1})$$

Update T

- Set $\gamma = 0.5$

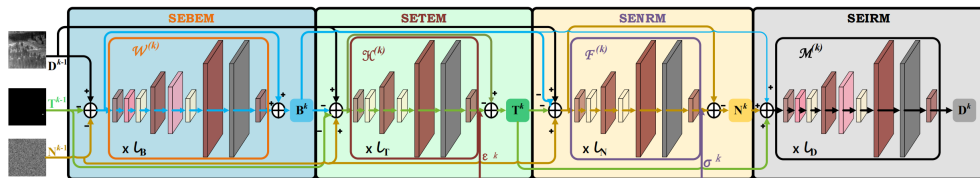
$$T^k = \gamma T^{k-1} + (1 - \gamma)(D^{k-1} - B^k - N^{k-1}) - \varepsilon \nabla \mathcal{S}(T^{k-1})$$

↓

$$T^k = T^{k-1} + D^{k-1} - B^k - N^{k-1} - \varepsilon \nabla \mathcal{S}(T^{k-1})$$

↓

$$T^k = T^{k-1} + D^{k-1} - B^k - N^{k-1} - \varepsilon^k \mathcal{H}^k(T^{k-1} + D^{k-1} - B^k - N^{k-1})$$



Update N

- Noise reduction module + squeeze-and-excitation network (SENRM)

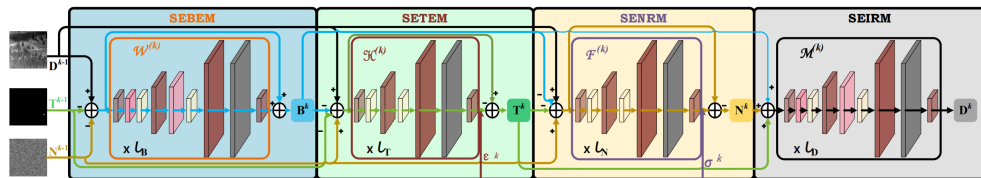
$$N^k = \arg \min_N \mu \mathcal{G}(N) + \frac{\alpha}{2} \|D^{k-1} - B^k - T^k - N\|_F^2$$

↓

$$N^k = \arg \min_N \frac{\mu L_N}{2} \|N - N^{k-1} + \frac{1}{L_N} \nabla \mathcal{G}(N^{k-1})\|_F^2 + \frac{\alpha}{2} \|D^{k-1} - B^k - T^k - N\|_F^2$$

↓

$$N^k = N^{k-1} + D^{k-1} - B^k - T^k - \sigma^k \mathcal{F}^k(N^{k-1} + D^{k-1} - B^k - T^k)$$



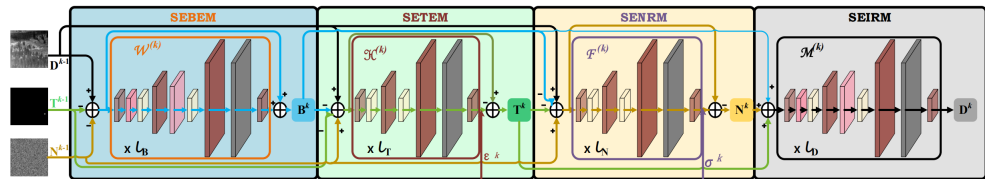
Update D

- ▶ Image reconstruction module + squeeze-and-excitation network (SEIRM)

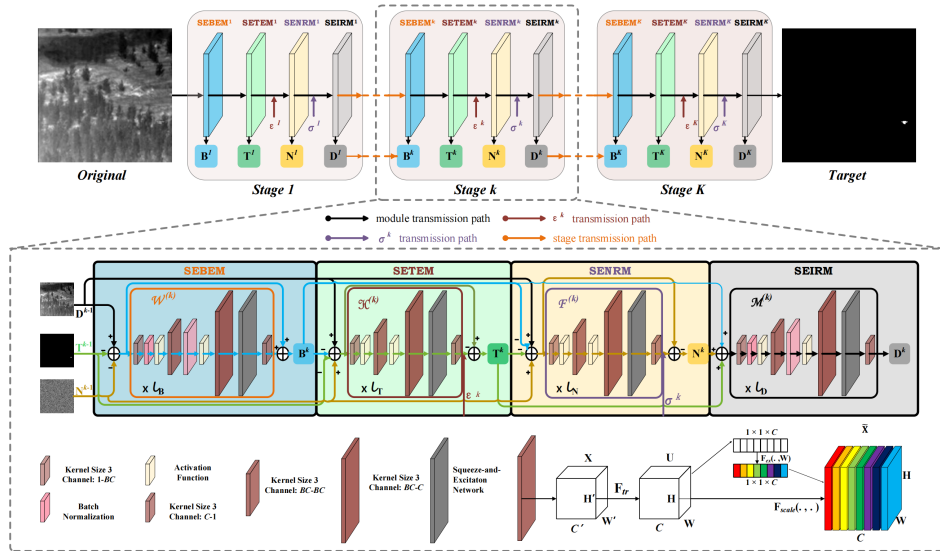
$$D^k = B^k + T^k + N^k$$

↓

$$D^k = \mathcal{M}^k(B^k + T^k + N^k)$$



Architecture



Experiments

- ▶ Compared methods
 - ▶ IPI: Gao-Meng-Yang et al, IEEE TIP, 2013
 - ▶ MPCM: Wei-You-Li, PR, 2016
 - ▶ PSTNN: Zhang-Peng, RS, 2019
 - ▶ AGPCNet: Zhang-Li-Cao et al, IEEE TAES, 2023
 - ▶ UIUNet: Wu-Hong-Chanussot, IEEE TIP, 2023
 - ▶ MSHNet: Liu-Liu-Zheng et al, CVPR, 2024
 - ▶ RPCANet: Wu-Zhang-Li et al, WACV, 2024
 - ▶ DRPCANet: Xiong-Zhou-Wu et al, IEEE TGRS, 2025
 - ▶ RPCANet++: Wu-Dai-Zhang et al, arXiv, 2025
- ▶ Evaluation metrics
 - ▶ Mean intersection over union ($mIoU \uparrow$), F_1 -score ($F_1 \uparrow$), Probability of detection ($P_d \uparrow$)
 - ▶ False alarm rate ($F_a \downarrow$)
- ▶ Loss function

$$\mathcal{L}_{\text{total}} = \mathcal{L}_{\text{segmentation}} + \eta \mathcal{L}_{\text{fidelity}} = \left(1 - \frac{1}{M_t} \sum_{i=1}^{M_t} \frac{\text{TP}}{\text{FP} + \text{TP} + \text{FN}} \right) + \frac{\eta}{M_t M} \sum_{i=1}^{M_t} \|D^K - D\|_F^2$$

Experiments

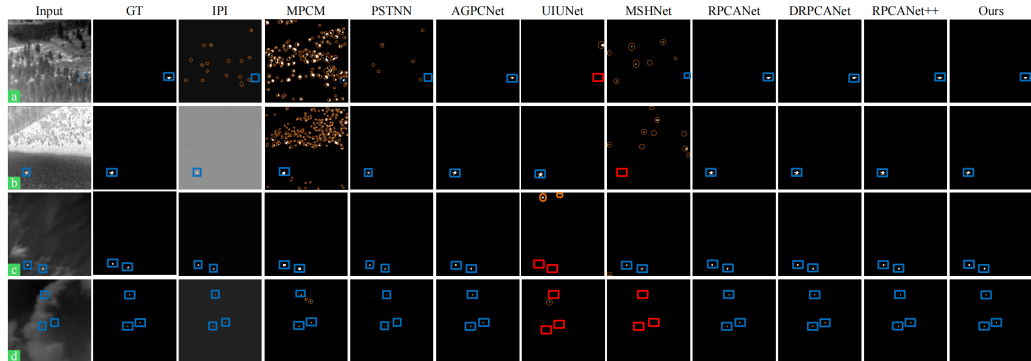
► Quantitative results

Methods	Params	NUDT-SIRST				SIRST-Aug				IRSTD-1k				Time (s) CPU/GPU
		mIoU ↑	F ₁ ↑	P _d ↑	F _a ↓	mIoU ↑	F ₁ ↑	P _d ↑	F _a ↓	mIoU ↑	F ₁ ↑	P _d ↑	F _a ↓	
IPI	–	34.83	51.49	92.58	7.14	21.90	35.97	80.36	2.20	18.67	31.48	78.54	11.11	3.0972/-
MPCM	–	25.96	40.78	78.59	7.91	19.49	33.00	93.58	3.04	14.81	25.93	69.03	6.51	0.0624/-
PSTNN	–	25.46	40.58	78.52	7.95	19.76	33.00	93.40	3.14	14.87	25.89	68.73	6.51	0.2249/-
AGPCNet	12.360M	85.31	92.45	97.90	4.77	72.36	83.83	99.03	35.56	61.00	75.75	89.35	5.34	-/0.0205
UIUNet	50.540M	88.71	94.01	91.43	1.89	71.80	83.59	98.35	28.29	63.06	77.35	93.60	6.57	-/0.0317
MSHNet	4.065M	89.99	93.57	96.07	2.63	71.64	84.16	90.78	23.09	64.50	77.55	91.68	4.46	-/0.0245
RPCANet	0.680M	89.31	94.35	97.14	2.87	72.54	84.08	98.21	34.14	63.21	77.45	88.31	4.39	-/0.0096
DRPCANet	1.169M	93.12	96.02	98.02	1.95	73.93	85.39	98.12	30.45	63.93	78.15	92.09	4.92	-/0.0101
RPCANet++	4.396M	92.46	96.05	98.05	1.44	73.14	84.39	97.36	32.48	64.03	77.26	89.35	4.28	-/0.0063
Ours	0.216M	92.37	96.54	98.41	1.79	74.56	85.43	99.17	29.78	64.68	78.55	89.39	4.66	-/0.0052

	NUDT-SIRST	SIRST-Aug	IRSTD-1k
#Size	256 × 256	256 × 256	512 × 512
#Training	663	8525	800
#Testing	662	545	201

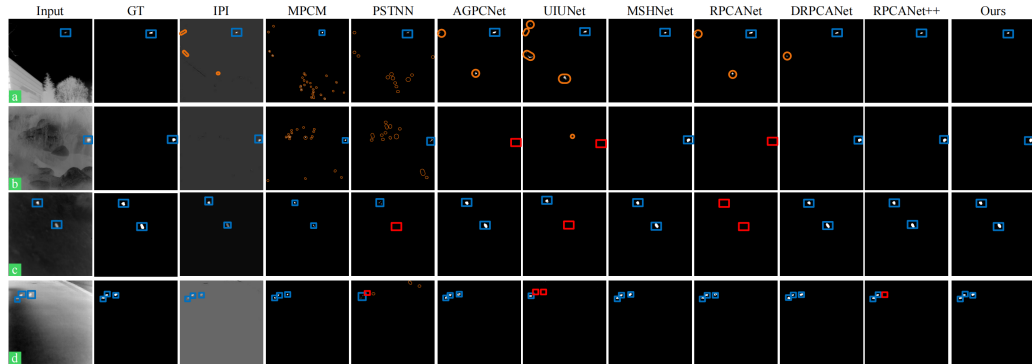
Experiments

► Visualization on NUDT-SIRST



Experiments

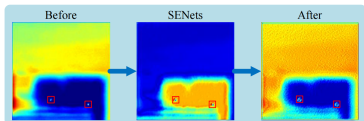
► Visualization on IRSTD-1k



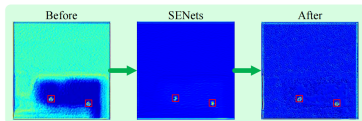
Experiments

► Ablation studies on SENets

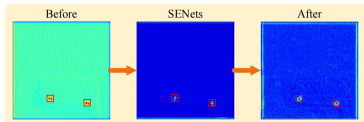
SENNets				NUDT-SIRST				SIRST-Aug				IRSTD-1k			
SEBEM	SETEM	SENRM	SEIRM	mIoU ↑	F ₁ ↑	P _d ↑	F _a ↓	mIoU ↑	F ₁ ↑	P _d ↑	F _a ↓	mIoU ↑	F ₁ ↑	P _d ↑	F _a ↓
✗	✗	✗	✗	73.56	78.45	79.36	8.56	60.75	70.28	81.24	43.67	50.26	61.34	70.57	15.95
✓	✗	✗	✗	80.57	81.39	86.35	5.68	65.96	75.37	86.99	39.82	55.84	65.26	76.36	11.12
✓	✓	✗	✗	88.36	89.45	90.18	4.00	70.17	80.78	93.17	34.78	60.56	72.58	83.70	8.10
✓	✓	✓	✗	91.14	96.06	97.18	2.05	73.27	84.45	98.07	27.73	63.58	77.53	88.71	3.95
✓	✓	✓	✓	92.37	96.54	98.41	1.79	74.56	85.43	99.17	29.78	64.68	78.55	89.39	4.66



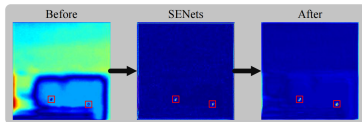
(a) SEBEM



(b) SETEM



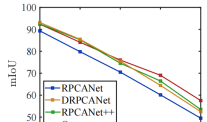
(c) SENRM



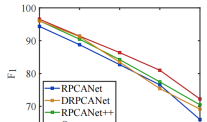
(d) SEIRM

Experiments

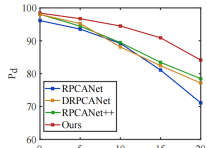
► Gaussian noise



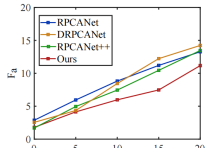
(a) mIoU



(b) F1

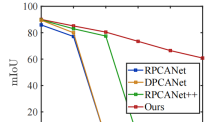


(c) Pd

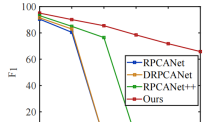


(d) Fa

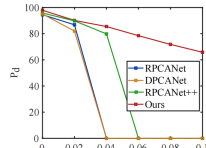
► Salt-and-pepper noise



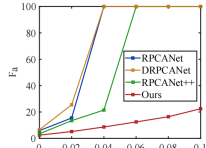
(a) mIoU



(b) F1



(c) Pd



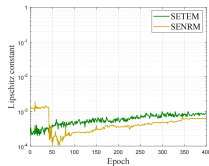
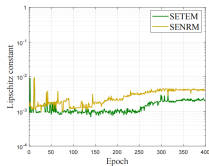
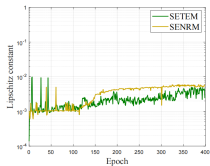
(d) Fa

Experiments

► Effects of the stage K

K	Params	NUDT-SIRST				SIRST-Aug				IRSTD-1k			
		mIoU ↑	F ₁ ↑	P _d ↑	F _a ↓	mIoU ↑	F ₁ ↑	P _d ↑	F _a ↓	mIoU ↑	F ₁ ↑	P _d ↑	F _a ↓
1	0.0360M	91.39	95.51	98.52	2.16	72.83	84.28	98.07	29.14	61.26	75.98	92.12	6.29
2	0.0720M	91.61	95.62	97.88	2.08	72.96	84.37	98.9	34.82	61.59	76.24	86.99	5.12
3	0.1080M	91.53	95.58	97.98	2.00	73.58	84.78	99.17	32.83	62.60	77.00	88.7	5.21
4	0.1439M	90.06	95.06	97.88	1.95	73.81	84.93	98.21	28.51	61.98	76.53	87.33	4.35
5	0.1799M	91.64	95.64	98.31	2.01	74.28	85.24	98.76	28.06	63.45	77.63	88.36	5.45
6	0.216M	92.37	96.04	98.41	1.79	74.56	85.43	99.17	29.78	64.68	78.55	89.39	4.66
7	0.2519M	88.53	93.58	96.77	3.74	72.29	83.92	98.9	27.38	62.29	76.76	87.33	4.82

► Lipschitz conditions



Outline

Introduction

Hyperspectral Denoising

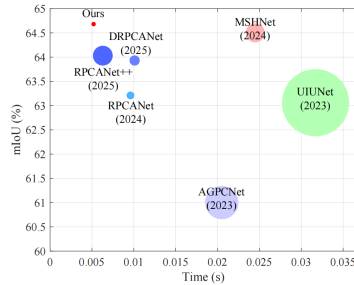
Infrared Small Target Detection

Conclusions

Conclusions

- ▶ Liu-Jin-Xiu et al, STAR-Net: An Interpretable Model-Aided Network for Remote Sensing Image Denoising, [Pattern Recognition](#), 172: 112496, 2026
- ▶ Liu-Han-Xiu et al, Lightweight Deep Unfolding Networks with Enhanced Robustness for Infrared Small Target Detection, [submitted to IEEE TIP](#), 2025

Methods	mIoU ↑	F ₁ ↑	P _d ↑	F _a ↓
IPI	25.13	39.65	83.83	6.81
PSTNN	20.03	33.16	80.22	5.87
MPCM	20.09	33.24	80.40	5.82
Ours	77.20	86.67	95.66	12.08



Thank you for your attention!

xcxiu@shu.edu.cn